JRC Scientific and Technical Reports

DONA detector: further improvements and evaluation for field applications

G. Lövestam, A. Fessler, J. Gasparro, M. Hult, P. Kockerols, G. Marissens, K. Okkinga and J.S.E. Wieslander

EUR 23305 EN - 2007

JRC EUROPEAN COMMISSION

irmm Institute for Reference Materials and Measurements

The mission of the IRMM is to promote a common and reliable European measurement system in support of EU policies.

European Commission
Joint Research Centre
Institute for Reference Materials and Measurements

Contact information
Address: G. Lövestam
Institute for Reference Materials and Measurements
Retieseweg 111
B-2440 Geel, Belgium
E-mail: goeran.loevestam@ec.europa.eu
Tel.: +32 (0)14 571 373
Fax: +32 (0)14 584 273

http://www.irmm.jrc.be/html/homepage.htm
http://www.jrc.ec.europa.eu

JRC 44684

EUR 23305 EN
ISBN 978-92-79-08813-1
ISSN 1018-5593

Luxembourg: Office for Official Publications of the European Communities

Printed in Belgium

1. Introduction

With the increasing number of nuclear installations it is essential to ensure that adequate techniques to monitor environmental neutron radiation and doses are available. Issues like environmental and personal safety, safety at work, benchmarking of existing monitoring techniques and unveiling of terrorist threats may be directly linked to whether neutron spectrometry is feasible. Today, practically only two techniques are used for measurement of environmental neutron energy spectra, Bonner sphere spectrometry [BR-60] which is rather accurate but bulky and time consuming to carry out, and bubble detectors [RO-87] which suffers from high uncertainties. Of the two, the Bonner sphere spectrometer is the by far most often used.

In this study, an alternative approach – the DONA detector, described in the IRMM exploratory research report [KO-05], is further tested. The technique used here is based on measuring the neutron activity induced in a series of metal disks, with different neutron excitation functions, followed by spectrum unfolding to obtain a complete neutron energy spectrum from the measurement site. A similar technique, usually referred to as the foil activation technique, is widely used to characterize high neutron fluence rates, for example inside nuclear reactors, see for example [NE-05]. The detector discussed here, however, is aimed for the measurement of much lower fluence rates which is facilitated by using thicker disks and low-background gamma-ray detectors for measuring the activation products.

For applications there are many situations where a better knowledge of the neutron spectrum would give a better understanding of the origin of the neutrons, scattering effects, possible shielding effects, etc. A few examples are the monitoring of neutron fluence at:

- containers and barrels containing unknown materials, for example in harbours and customs control stations,
- neutron and nuclear physics laboratories,
- nuclear accelerators,
- neutron reactors,
- fusion research installations,
- medical installations for treatments using neutrons,
- flights and satellites,
- accidents involving nuclear materials.

2. DONA detector, principle of operation

As the principle of the DONA detector already has been discussed in the previous report [KO-05] only a brief description is given here. The DONA detector system consists of three parts; 1) the neutron sensitive device consisting of a series of metal disks, 2) a gamma-ray measurement station, and 3) the data evaluation station. As the neutron sensitive device does not require any electronics or data acquisition system on the measurement site, this arrangement constitutes a great advantage as no delicate equipment has to be brought out in the field. On the contrary, the precise activation measurements can be done in an established gamma measurement laboratory.

A neutron spectrometry field measurement is consequently done in three steps as illustrated in figure 1. In the first step the detector device is positioned at the site of measurement. Either a "static measurement programme" is followed, i.e. detectors are always positioned at locations where possible neutron radiation could occur, for example following an accident event, and the detectors are collected for measurements only when a neutron irradiation is suspected, or a "dynamic measurement programme" is used where the detectors are positioned in a suspected neutron field only at a certain occasion and for a certain pre-defined time. Typical irradiation times are, naturally, dependent on the neutron fluence rate, but for fluence rates of ~100 neutrons/(cm^2 s) about 24 h should be foreseen.

The choice of measurement programme is, of course, dependent on the activities at the measurement sites and the character of the expected neutron fields, but a dynamic measurement programme is generally easier to evaluate as the time information for the irradiation and possible fluence rate variations is normally better known.

In the second step, the detector device is transported to the gamma measurement laboratory where the neutron induced activity of every disk and isotope is measured. The transportation is critical as it should be done within one or two half life periods of the isotope with the shortest half life.

In the third step, the data from the gamma measurements is evaluated using a few channel spectrum unfolding technique to obtain the measured neutron energy spectrum.

Step 1, Irradiation at measurement site

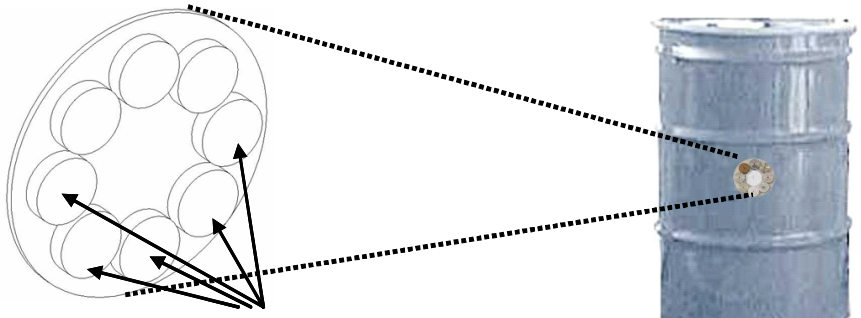

Step 2. Gamma measurements in laboratory

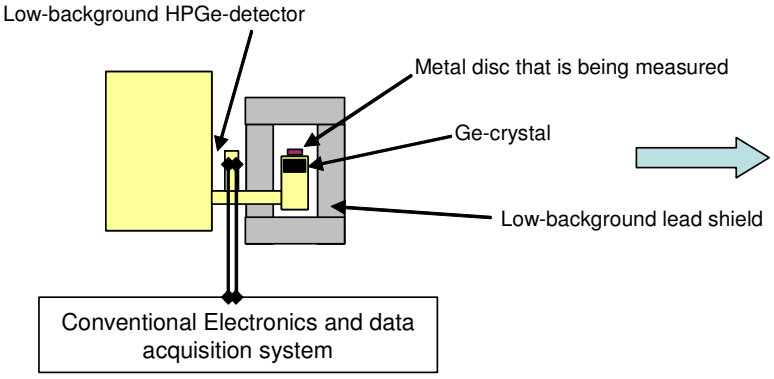

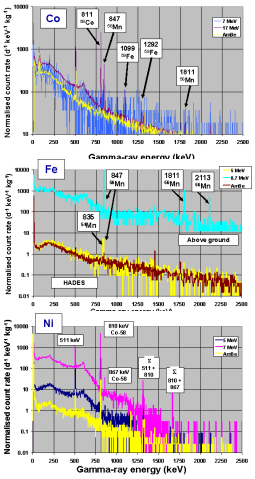

Step 3. Spectrum unfolding

Radionuclide	Saturation activity (mBq)
56Co	50
55Mn	23
60Co	40
64Cu	112
etc.	...
...	...
...	...

Input to the unfolding: "Disc activities"

Spectrum unfolding

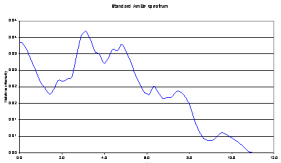

The final result: A neutron energy intensity spectrum

Figure 1. Schematic representation of a neutron fluence spectrum measurement sequence using the DONA detector.

3. Materials and Methods

In summery, the following results were obtained from the first DONA exploratory research project [KO-05]:

- From the study of 260 different nuclear reactions, 8 materials were selected as optimal for the detector.
- Five neutron test irradiations were performed in quasi mono-energetic neutron fields of 5, 7, 8, 8.7 and 17 MeV at the IRMM Van de Graaff accelerator laboratory and one irradiation with an AmBe source (broad neutron spectrum) at the Belgian nuclear research centre SCK•CEN in Mol.
- The spectra obtained from the disk activations and the following unfolding showed good agreement with spectra simulated using Monte Carlo and neutron kinematics calculations, and as measured using a Bonner Sphere system.
- Low-level (LGS) and ultra-low level gamma spectrometry (ULGS) of the activated disks facilitated measurements of very low neutron fluences with detection limits for fast neutrons in the order of 10 neutrons/(s·cm^2) (ULGS) and 250 neutrons/(s·cm^2) (LGS), respectively.

These results were used for this study to further:

- fine tune and improve the technique, also for neutrons below 500 keV, and
- evaluate and test its performance in real field applications.

3.1 Improving the technique

For the fine tuning of the DONA detector performance the following improvements have been made:

- Au has been included and evaluated as monitor for neutrons with energies < 500 keV.
- Several excitation functions have been added to the response function data file.
- The cross section data file has been changed from RNAL (IAEA) to the International reactor dosimetry file, IRDF-2002 (http://www-nds.iaea.or.at/irdf2002/) (IAEA), when data has been available in this file.
- The software routine, WinDONA, for the unfolding of neutron spectra has been considerably improved.
- A library of IAEA environmental neutron spectra are now included as default spectra for unfolding [IA-01].

In the first study the ^{115}In(n,γ)^{116m}In reaction was used to monitor neutrons in the energy region < 500 keV. Since the excitation function contains a resonance area in the low energy region, the cross section data in the lowest energy bin had to be averaged to a mean value. This approximation was believed not being very accurate and alternative reactions in the energy region were tested. Also, a stack of disks (1 mm/disk) arranged as Au-Cd-Au-Cd in the centre of the detector, has been tested so as to make use of the Cd-difference technique. Cd has a rather sharp increasing cross section for neutrons < 1 eV. In total, the low neutron energy reactions in Table 1 are now included in the DONA data base file:

Reaction	Cross section data base
Cu63(n,γ)Cu64	Irdf-2002
In115(n, γ)In116m	Irdf-2002
Ta181(n, γ)Ta182	Irdf-2002
Au197(n, γ)Au198	Irdf-2002
natCd(n,tot)	Irdf-2002
Au197(n, γ)Au198,Cd-shield	Irdf-2002

Table 1. The low neutron energy reactions now included in the DONA data base file.

In addition, in Table 2 is the included threshold reaction cross section data:

Reaction	Cross section data base
Mg24(n,p)Na24	Irdf-2002
Al27(n,p)Mg27	Irdf-2002
Al27(n,a)Na24	Irdf-2002
Ti46(n,p)Sc46	Irdf-2002
Ti47(n,p)Sc47	Irdf-2002
Ti48(n,p)Sc48	Irdf-2002
Fe54(n,p)Mn54	Irdf-2002
Fe56(n,p)Mn56	Irdf-2002
Ni58(n,p)Co58	Irdf-2002
Ni58(n,2n)Ni57	Irdf-2002
Ni58(n,d+np)Co57	RNLA
Co59(n,a)Mn56	Irdf-2002
Co59(n,2n)Co58	Irdf-2002
Co59(n,p)Fe59	ENDF
Cu63(n,a)Co60	Irdf-2002
Cu65(n,2n)Cu64	Irdf-2002
In113(n,n')In113	EXFOR
In115(n,n')In115	Irdf-2002
In115(n,2n)In114m	Irdf-2002
Ti46(n,p)Sc46+Ti47(n,np+d)Sc46	Irdf-2002
Ti47(n,p)Sc47+Ti48(n,np+d)Sc47	Irdf-2002
Nb93(n,2n)Nb92	Irdf-2002
Zr90(n,2n)Zr89	Irdf-2002
Zr96(n,2n)Zr95	RNLA
Au197(n,2n)Au196	Irdf-2002
Ti46(n,p)Sc46+Ti47(n,np)Sc46	Irdf-2002
Ti47(n,p)Sc47+Ti48(n,np)Sc47	Irdf-2002
Ti47(n,np+d)Sc46	RNLA
Ti47(n,np)Sc46	Irdf-2002
Ti48(n,d)Sc47	RNLA
Ti48(n,np)Sc47	Irdf-2002

Table 2. The threshold reaction cross section data.

All spectra are interpolated to a linear scale in 200 bins from 0 to 20.0 MeV, see Appendix 1. The interpolation has been done using spline interpolation.

For the unfolding software, WinDONA, the IAEA environmental neutron spectra have now been included as default spectra data base. This opens for a novel approach for few channel spectrum unfolding. Instead of using one specified default spectrum, a sequence of spectra is tested and the spectrum giving the lowest chi-2 value is chosen as default spectrum. The data base contains more than 400 spectra all represented as neutron fluence in 60 energy bins per unit lethargy ($\ln(E_{i+1}) - \ln(E_i)$), see appendix 2. The WinDONA software was adapted to the structure of the data base so as the original structure was kept in order to facilitate easy downloading of upgrades from the IAEA homepage. However, prior to unfolding, all default spectra are re-binned by WinDONA to a 200 bins linear binning structure from 1-20 MeV.

3.2 Test at calibrated neutron source and field application

DONA detectors were tested at two occasions 1) in a calibrated and certified ^{252}Cf neutron field at Physicalish Technische Bundesanstalt, PTB, in Brauncshweig and at the Belgonucleaire MOX fuel manufacturing site in Dessel, Belgium. For the calibration at PTB the DONA detector was positioned at a distance of 500 mm from the central disk of the detector to the centre of the source, in 0 degrees angle. The irradiation time was 86,400 s with a direct fluence field of 7791±99 neutrons/(cm^2 s) and an in-scattering field of 633±43 (7.51±0.46 %).

MOX is the abbreviation for Mixed Oxide, a fuel for nuclear power plants that consists of a mixture of depleted uranium oxide and plutonium oxide. MOX fuel recovers plutonium produced in all reactors and uses depleted uranium which is a sub-product of the uranium enrichment process. The recovering of plutonium in MOX elements reduces the quantity of plutonium produced in nuclear power plants and economizes uranium ore needs. Belgonucleaire's plant produced till 2006 yearly about 35 to 38 tons of MOX fuel rods.

The fuel rods are stored in metal fuel container boxes which in turn are positioned in a concrete bunker. The neutron radiation of the MOX fuel is generated by spontaneous fissions of some plutonium nuclides and by (α, n) reactions with the oxygen nuclei. For this study, one box was taken out of the bunker and two detectors were positioned at the top of the container box; one on top and at the centre of the box and the other on top and the side of the box. The detectors were irradiated for 48 h.

3.3 Activation measurements

The activity induced in the pure metal disks for all detectors was measured using low-level and ultra low-level gamma-ray spectrometry. A low-level gamma spectrometry includes an HPGe-detector made from selected radio pure materials and installed in a specially designed radio pure lead shield. In ultra low-level gamma spectrometry additional measures such as using a muon shield or an underground laboratory are taken.

The main principles governing the choice of materials were discussed in the first DONA report, where it was concluded that to obtain low detection limits for fast neutrons it is essential that relatively large amounts of the material is activated. This implies the use of thick foils or disks instead of the thin foils that are commonly used for thermal neutrons. For thicker disks, it is not useful to measure the beta-particles in a beta-gamma spectrometer since only the beta particles from the outer part of the disk will enter the beta-counter. Dissolving disks and measure using liquid scintillation counting or other methods is not an option since DONA requires a method with very simple sample preparation. Gamma-ray spectrometry has the advantages of normally requiring very little sample preparation and the actual measurement is easy to carry out. In case special low-background or ultra low-background gamma detection systems are used, the detection limits can be very low (μBq/kg). In recent years there has been a significant improvement of HPGe-detector performance [HU-05], which in combination with the use of underground laboratories has triggered new fields of gamma spectrometry. Figure 2 shows the background spectrum in the underground laboratory HADES in comparison with a state-of-the-art detector above ground.

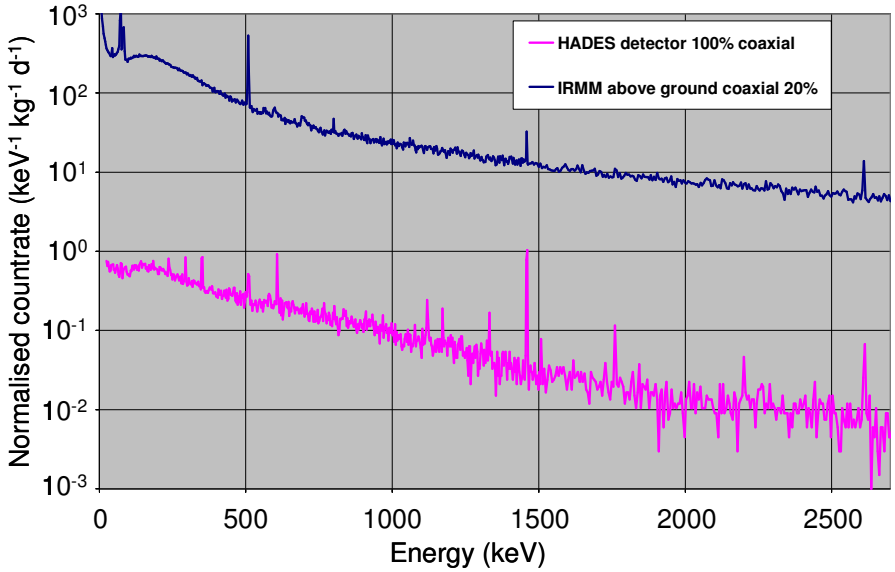

Figure 2. The background spectra for one HPGe-detector located in HADES and another above ground. The count rate is normalised to the mass of the Ge-crystal.

All disks used in this study were already available at IRMM, in the Van de Graaff building and in the radionuclide metrology laboratory. As tritium is a plausible contaminant in the Van de Graaff building disks were checked for possible contamination but no tritium was detected. Also, disks were measured using low-level gamma spectrometry prior to activation. The only activity measured was from small amounts of ^{60}Co (250 mBq/kg) in the copper disks. Hence, it was decided not to use ^{60}Co in copper disks in the DONA data evaluation.

Table 3 gives details of the HPGe-detectors used for the measurements. All measurements were carried out either in the underground laboratory HADES or above ground at IRMM.

Detector	Relative efficiency (%)	Crystal mass (kg)	Crystal configuration	Dead layer thickness (mm)	Window material and thickness (mm)	Location
Ge-2	8	0.209	Semi-planar	0.0005	0.7 mm, Al	HADES
Ge-3	60	1.337	Coaxial	1	0.7 mm, Al	HADES
Ge-4	106	2.195	Coaxial	0.0005	0.5 mm, Al	HADES
Ge-5	50	0.803	Planar	0.002	1.0 mm, Al	HADES
Ge-6	80	2.106	Coaxial	0.7	1.0 mm, Cu	HADES
Ge-7	80	2.106	Coaxial	0.0005	1.5 mm, Al	HADES
Ge-8	19	0.385	Coaxial	0.7	1.5 mm, Al	HADES
Ge-T2	20	0.423	Coaxial	0.7	1.5 mm, Al	IRMM

Table 3. Data for the HPGe-detectors used for the gamma measurements.

After collecting the detectors at the respective activation site, the disks were placed in Teflon containers. The Teflon containers used for HADES measurement have been specially designed for underground low-level measurements. The containers can be closed with a lid and an O-ring seal. In this study it was not essential to have equilibrium between radon-daughters coming from the sample so in most cases the lid was not used. The Teflon containers were placed directly on the end cap of an HPGe-detector or in some cases on a so called centring ring in order to have the container and the disk centred on the detector.

The gamma spectra net peak areas, C, were determined using manual subtraction of the background, calculated from a region of interest around the respective peak. The massic activity, *a*, was calculated using the formula:

$$a = \frac{C\lambda}{(1-e^{-\lambda t_m})P_\gamma \varepsilon_{\mathrm{Re}f}} \frac{1}{m} \xi e^{-\lambda t_d}$$

C = Number of net-counts in the peak of interest.
λ= Decay constant for radionuclide of interest.
t_m = Measurement time.
t_d = Decay time from reference date to measurement date.
ε_{Ref} = Full energy peak efficiency per γ-ray of the γ-ray peak in question, derived from measuring a reference sample.
m = Mass of the sample.
P_γ = Gamma-ray emission probability.
ξ = Efficiency correction factor.

The efficiency correction factor ξ is simply the ratio of the efficiencies calculated using a Monte Carlo code for the reference disk and the real disk. However, in this study reference samples were not available for all radionuclides. In such cases the factor ξ was set to unity and the full energy peak efficiency, calculated using the EGS4 Monte Carlo code [NE-85] based on the geometry of the sample itself, was used for the factor ε_{Ref}.

When performing a DONA measurement it is very practical to have one HPGe-detector for every activation disk. When many disks are used (as in this case) this is not always possible. A thorough planning of a measurement is, thus, instrumental. The following points should be considered:

- To start the measurement of disks with short-lived radionuclides first.
- To measure each disk on an appropriate detector, i.e. the low energy gamma rays should be measured on a small Ge-crystal with a thin dead layer, whilst high energy gamma-rays should be measured on a big Ge-crystal.
- To collect several spectra from the same disk since there might be short-lived radionuclides as well as long lived. In such cases it may be an option to measure a disk a second time at a later occasion.

It should, however, be pointed out that in order to minimise the uncertainty in the subsequent unfolding process, it is an advantage to measure all disks using the same HPGe detector.

The activity results given in this report (table 3 and 4 below) are decay corrected and the activity refers to the day and time when the respective activation was stopped. The dominating uncertainty contributions come from detector efficiency and counting statistics. The uncertainty of the detector efficiency is 3% due mainly to uncertainties in the geometrical description of the detector as well as photon and electron interaction cross-sections [NE-00]. The expressed uncertainties are given as the combined standard uncertainty estimated following the ISO/BIPM Guide to the Expression of Uncertainty in Measurement [IS-95]. Nuclear decay data is taken from the PC based interactive database Nucléide V.2.0, supplied by DAMRI/LPRI [DA-98]. With the entity "massic activity" it is meant the activity divided by the mass of the complete sample (here: disk-mass). The entity "specific activity" is the activity of a certain radionuclide divided by the mass of the isotope from which it was produced.

Correction factors for self shielding and multiple scattering effects, as well as for scattering from neighbouring disks was done using MCNP-4C2 [BR-93]. In table 2 and table 3 the corrected specific saturation activity is given, here multiplied with the activation time factor $\left(1-e^{-\lambda \cdot t_{irr}}\right)^{-1}$, where t_{irr} is the irradiation time and λ is the decay constant.

3.4 Spectrum unfolding

A critical part of a DONA measurement is the spectrum unfolding. The unfolding is used to calculate a neutron energy spectrum of, for example, 100 energy bins from the limited number of measured reaction activities, normally 6-20. The discrete equation to solve is:

$$N_k + \varepsilon_k = \sum_i \sigma_{ki} \Phi_i \quad k = 1, n;\ i = 1,100;\ n = 6\,to\,20$$

where N_k is the measured activation data of reaction k, ε_k the uncertainty in the activation data, σ_{ki} the reaction cross sections of the individual neutron energy channels (response function) and Φ_i the sought energy spectrum. The response function, $\sigma_{ki,}$ containing neutron activation cross sections must be accurately known for the included materials. Following the spectrum unfolding the absolute neutron fluence for the exposure time can be calculated using conventional techniques.

In this second part of the DONA project the Gravel unfolding code was used [JA-80]. In the first part the Maxed code [Re-02], based on the maximum entropy technique was used, but as the Maxed code has a considerably longer execution time it can not be used for, for example, searching of best default functions as discussed above. In addition, the two codes give normally similar results.

The Gravel code, which is an extension of the more well known SAND-II code, is an iterative code for which, given an initial estimate of the neutron spectrum (*J*), the next iteration (*J+1*) spectrum is calculated as:

$$\Phi_i^{J+1} = \Phi_i^J \exp\left(\frac{\sum_k W_{ik}^J \log\left(\frac{N_k}{\sum_{i'} \sigma_{ki'} \Phi_{i'}^J} \right)}{\sum_k W_{ik}^J} \right) \quad ; where \quad W_{ik}^J = \frac{\sigma_{ki} \Phi_i^J}{\sum_{i'} \sigma_{ki'} \Phi_{i'}^J} \frac{N_k^2}{s_k^2}$$

In the formula *s* denotes the standard deviation. The procedure executes fast on a normal PC, is rather stable and gives always a non-negative spectrum as a result. However, how the solution spectrum relates to the initial estimate of the spectrum, i.e. the default spectrum, is obscure. Also, standard sensitivity analyses and uncertainty propagation is not possible.

The stopping criterion for iterations is either that a pre-set maximum number of iterations has been calculated or a pre-set chi-2 value has been obtained:

$$\chi_{n-1}^2 \sim \frac{\sum_k^n \left(\sum_i^m \sigma_{ki} \Phi_i - A_k \right)^2}{s^2}$$

For all measurements in this study the preset chi-2 value was set to 1.0. In no case, the pre-set number of iterations was reached.

4. Results and Discussion

Table 4 gives the measured gamma data for the test irradiation at the PTB ^{252}Cf source.

	Reaction	Specific activity *10^24	Uncertainty
	Al27(n,a)Na24	8.130E+00	6.5%
	In115(n,n')In115	1.729E+03	2.1%
	In115(n,g)In116m	6.796E+03	2.0%
	In115(n,2n)In114m	3.550E+03	7.3%
	In113(n,n')In113	1.413E+03	12.1%
	Co59(n,a)Mn56	1.824E+00	15.1%
	Co59(n,2n)Co58	2.676E+00	11.1%
	Co59(n,p)Fe59	1.180E+01	4.6%
	Fe54(n,p)Mn54	4.442E+02	7.4%
	Fe56(n,p)Mn56	1.393E+01	7.1%
	Mg24(n,p)Na24	1.967E+01	5.7%
	Ti46(n,p)Sc46	6.240E+01	11.4%
	Ti47(n,p)Sc47	1.613E+02	5.5%
	Ti48(n,p)Sc48	2.218E+00	9.1%
	Ni58(n,p)Co58	9.429E+02	4.3%
	Zr90(n,2n)Zr89	1.119E+00	20.3%
	Zr96(n,2n)Zr95	2.792E+02	9.2%
Au-14 foil	Au197(n,g)Au198,Cd-shield	5.539E+03	2.1%
Au-41 disc	Au197(n,2n)Au196	3.626E+01	5.6%
	Au197(n,g)Au198	5.597E+03	2.2%

Table 4. Measured gamma data from the irradiation in the PTB ^{252}Cf neutron calibration facility. The specific activity is given in Bq per atom at the end of irradiation. Grayed reactions are not used in the unfolding.

Data from in total 20 reactions were measured. The result from the unfolding when including all data, and using the PTB ^{252}Cf model spectrum as default spectrum, gives a final chi-2 value of 352.0 indicating that some data or cross sections are obscure. The corresponding chi-2 value for the default spectrum is 560.4. The WinDONA function "optimize" tests all data to find those that contribute most to the chi-2 value. When the data indicated with grey text in table 2 are excluded from the input data set, a chi-2 value of 0.943 is obtained, below the pre-set value of 1.0. The corresponding chi-2 value for the default spectrum is 502.4. The reason why some data have to be excluded is not known but a plausible explanation is that the used excitation function data is not correct. Nevertheless, by including 13 reactions a very low chi-2 value is obtained.

Figure 3 displays the 13 included excitation functions and figure 4 the unfolded spectrum together with the ^{252}Cf model spectrum from PTB. As can be seen from figure 4, the model spectrum is very well represented by the results from the DONA detector measurement.

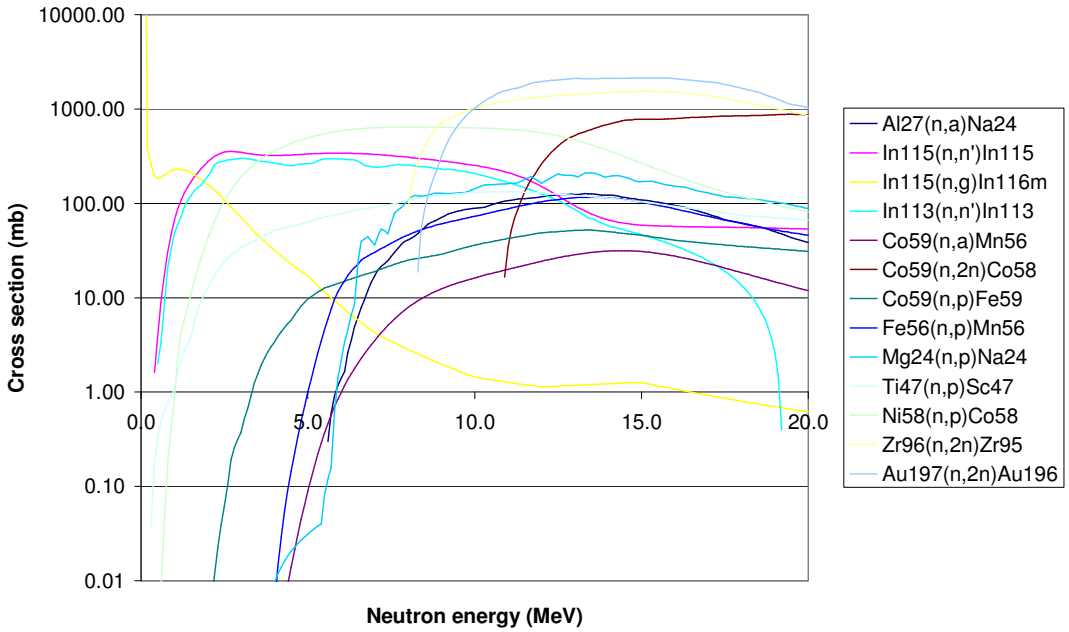

Figure 3. The excitation functions included in the measurement at the PTB ^{252}Cf source.

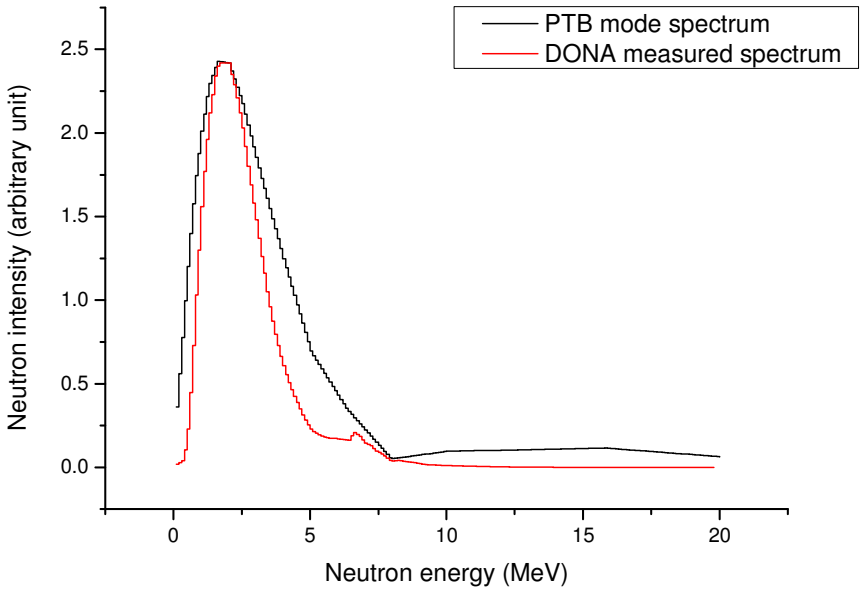

Figure 4. Unfolded spectrum (red curve) measured with the DONA detector at the PTB ^{252}Cf source. The black spectrum is the PTB model spectrum for a ^{252}Cf source.

The results for the measurement of the MOX fuels are given in Table 5 below.

Reaction	Detector 1 Specific activity	Uncertainty	Detector 2 Specific activity	Uncertainty
Ti46(n,p)Sc46+Ti47(n,np+d)Sc46	1.55E-25	3.96E-26	2.35E-25	1.21E-25
Ti47(n,p)Sc47+Ti48(n,np+d)Sc47	1.18E-23	5.73E-25		
Ti48(n,p)Sc48	9.57E-26	1.13E-26	1.34E-25	2.41E-26
Fe54(n,p)Mn54	8.10E-25	7.36E-26	6.25E-25	6.16E-26
Fe56(n,p)Mn56				
Ni58(n,p)Co58	3.71E-24	1.57E-25	4.36E-24	1.83E-25
Ta181(n,γ)Ta182	1.24E-22	3.26E-24		
Co59(n,p)Fe59			6.46E-26	1.73E-26
In115(n,n')In115	2.79E-22	1.28E-23	3.35E-22	1.49E-23
In115(n,g)In116*	2.96E-21	7.57E-23	2.89E-21	7.26E-23
In113(n,n')In113	2.31E-22	5.70E-23	2.60E-22	5.26E-23
Mg24(n,p)Na24	6.89E-25	9.20E-26		
Au197(n,γ)Au198	2.88E-21	1.15E-22	3.04E-21	1.22E-22

Table 5. Measured data from the irradiation at the Belgonucleaire MOX fuel fabrication site. The specific activity is given in Bq per atom at the end of irradiation. Grayed reaction data are not used in the unfolding. Detector 1 was positioned at the top but to the side of the fuel container and detector 2 at top and centre of the container.

Again the WinDONA "optimize" function was used to sort out data that contribute most to the chi-2 value calculated by the unfolding routine. The corresponding remaining excitation functions are displayed in figure 5. Obviously, a good overlap is achieved with the remaining data set. The corresponding unfolded spectra are displayed in figure 6.

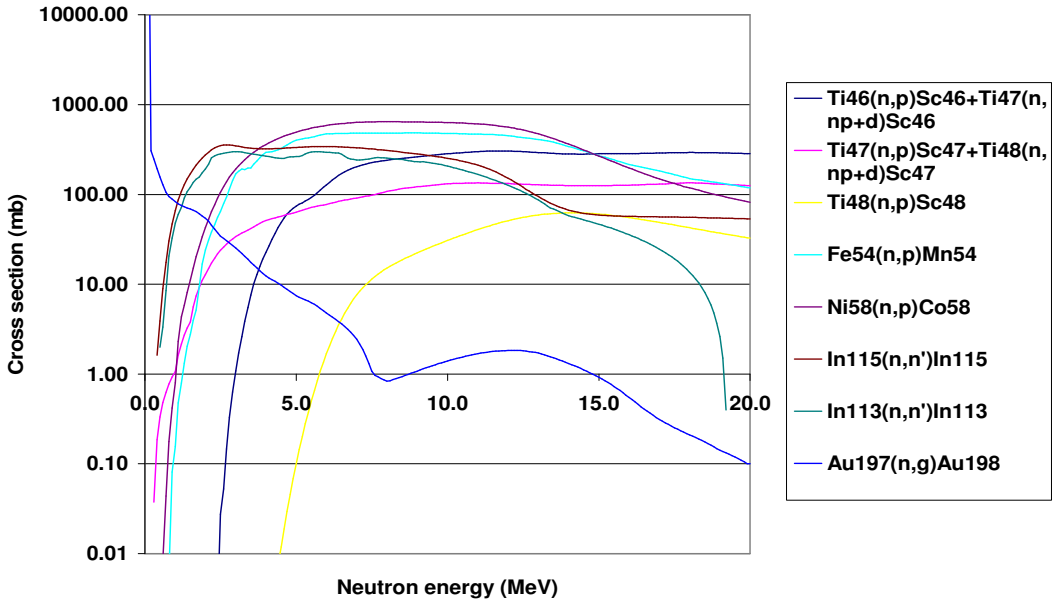

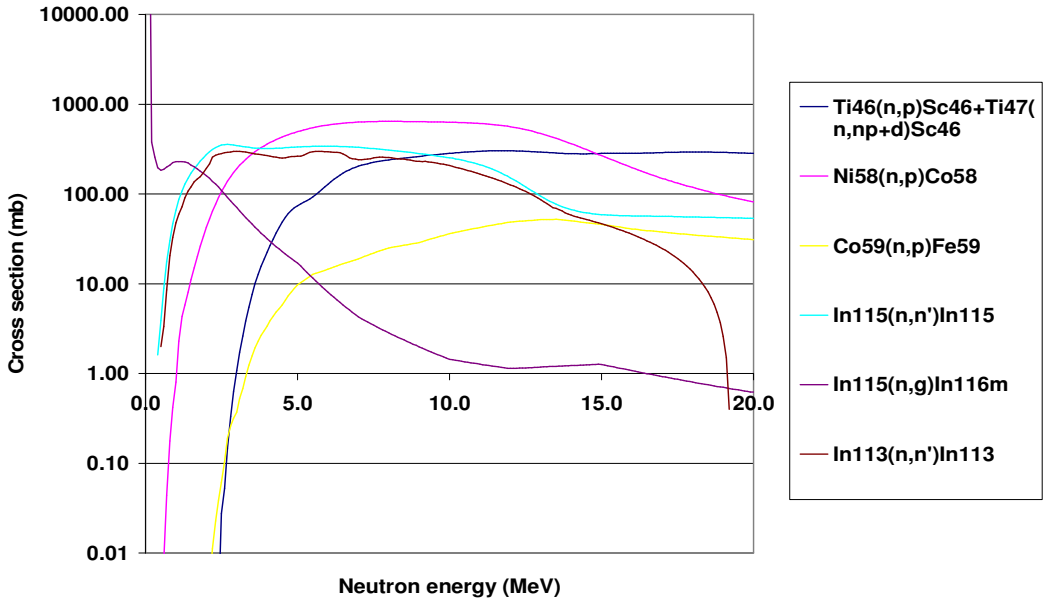

Figure 5. The excitation functions included in the DONA measurement of the MOX fuel container position 1 (upper) and position 2 (lower).

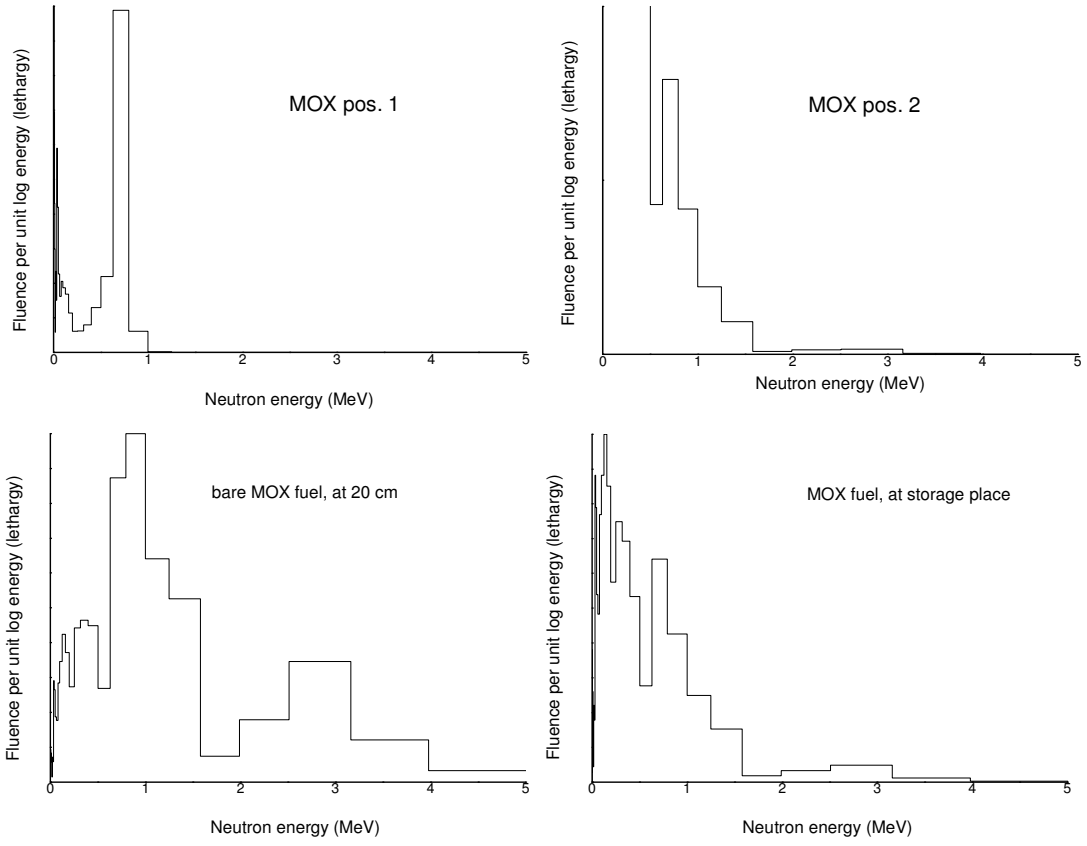

Figure 6. Unfolded spectra from the measurements at the MOX fuel fabrication site Belgonucleaire (upper) and MOX fuel spectra from the IAEA operational neutron fluence spectra library (lower). Position 1 is at the top of the container but close to the left short side edge while position 2 is at the top of the container in the centre.

Figure 6 shows that the measured spectra correspond well with the MOX fuel spectrum from the storage place but less with the bare MOX fuel spectrum. This is expected as the fuel container is shielded. For the measurement at position 1 (short side of the container) no spectral component is measured above 1.5 MeV while this can be clearly seen for the measurement at the centre of the container (position 2), although less intense than for the IAEA MOX fuel at storage place spectrum. This spectrum has also a considerable low energy component which is, again, believed to be an effect of shielding.

5. Conclusions and future prospects

The measurement in environmental neutron fluence fields presented here show that the DONA detector can be used also in low fluence rate environment. As such, it is a good candidate for being an attractive alternative to the considerably more bulky Bonner sphere spectrometer. Indeed, as an environmental neutron-fluence detector, the detector possesses a number of distinct advantages. The detector

- is only sensitive to neutron radiation,
- is small and robust,
- requires no electrical power at the neutron fluence measurement site,
- can be placed at remote locations or locations with difficult access and/or in hazardous environments,
- sensitivity can be increased by using more and bigger disks and by using underground gamma-ray detectors for measuring the activity in the disks,
- is energy sensitive over a large neutron energy interval, and
- is of relative low cost.

A few limitations may, however, also be noted:

- The measurement of the activation products can be time-consuming, especially if low detection limits are sought.
- The necessary time between the end of the activation and the start of the gamma-ray measurements limits the possible disk materials to isotopes with long half-lives relative to the transport time.
- Only constant neutron fields can be accurately measured, no information is obtained about fluence rate-changes in the spectrum during the irradiation time.

The DONA detector system will be further exploited and developed to a commercial prototype. The project was granted 55,000 € following an application for the JRC-TTSC Innovation Project Competition 2007. This project includes the following tasks:

1. Design and realisation of a detector holder industrial prototype.
2. Design and realisation of a dedicated gamma measurement station industrial prototype.
3. Adoption and testing of developed software to a user friendly programme package.
4. Definition of a complete detector concept device for commercialisation.
5. Definition of way of commercialisation and market research.

Acknowledgements

The HADES personnel of SCK•CEN are gratefully acknowledged for their assistance. Maurice Vanuytven assisted at the irradiations at Belgonucleaire. Hamid Tagziria (EC-JRC-IPSC) made the Monte Carlo calculations of neutron transport using the MCNP-4C2 code.

References

[BR-60] R.L. Bramblett, R.I. Ewing and T.W. Bonner, A new type of neutron spectrometer. Nucl. Instr. and Meth. 9, 1-12, 1960.

[BR-93] Briesmeister J.F., editor. (1993) MCNP - A General Monte Carlo N-Particle Transport Code, Version 4A. LA-12625, Los Alamos, USA.

[DA-98] DAMRI/LPRI (1998) Nuclear Decay Data - Nucléide Version 2.0. B019 Gif-sur-Yvette, France.

[HU-05] Hult M, Preusse W. and Gasparro J "Underground Gamma-ray Spectrometry" Submitted for publication to Acta Chimica Slovenica.

[IA-01] IAEA – Compendium of Neutron Spectra and Detector Responses for Radiation Protection Purposes, Technical Report Series 403 (2001).

[IS-95] ISO (1995) Guide to the Expression of Uncertainty in Measurement. 1st edition corrected version. ISBN 92-67-10188-9. International Organization for Standardization, Geneva, Switzerland.

[JA-80] G. Jacobs and R. van den Bosch, Calibration measurements with the multisphere and neutron spectrum analyses using the SAND-II program, Nucl. Instr. And Meth. 175 (1980) 483-489.

[KO-05] P.Kockerols, A.Fessler, J.Gasparro, M.Hult, G.Lövestam, K.Okkinga, Neutron spectrometry and dosimetry using the activation technique (DONA) - a feasibility study, IRMM internal report, RS/51/05, 2005.

[NE-85] Nelson, W.R., Hirayama, H., Rogers, D.W.O. (1985) The EGS4 code system. SLAC Report 265.

[NE-00] Nelson, W.R (2000) Private communication.

[NE-05] C. Negoita, Measurement of Neutron Flux Spectra in a Tungsten Benchmark by Neutron Foil Activation Method, Theses, Shaker Verlag, Aachen Germany, ISBN 3-8322-3519-1, 2004.

[RE-02] M. Reginatto, P. Goldhagen, S. Neumann, Spectrum unfolding, sensitivity analysis and propagation of uncertainties with the maximum entropy code MAXED, Nucl. Instr. And Meth. A 476 (2002) 242-246.

[RO-87] S.C. Roy, R.E. Apfel, Y.-C. Lo, Superheated drop detector: A potential tool in neutron research. Nucl. Inst. and Meth. A255, 199, 1987.

Appendix 1

Excitation functions included in WinDONA for spectrum unfolding.

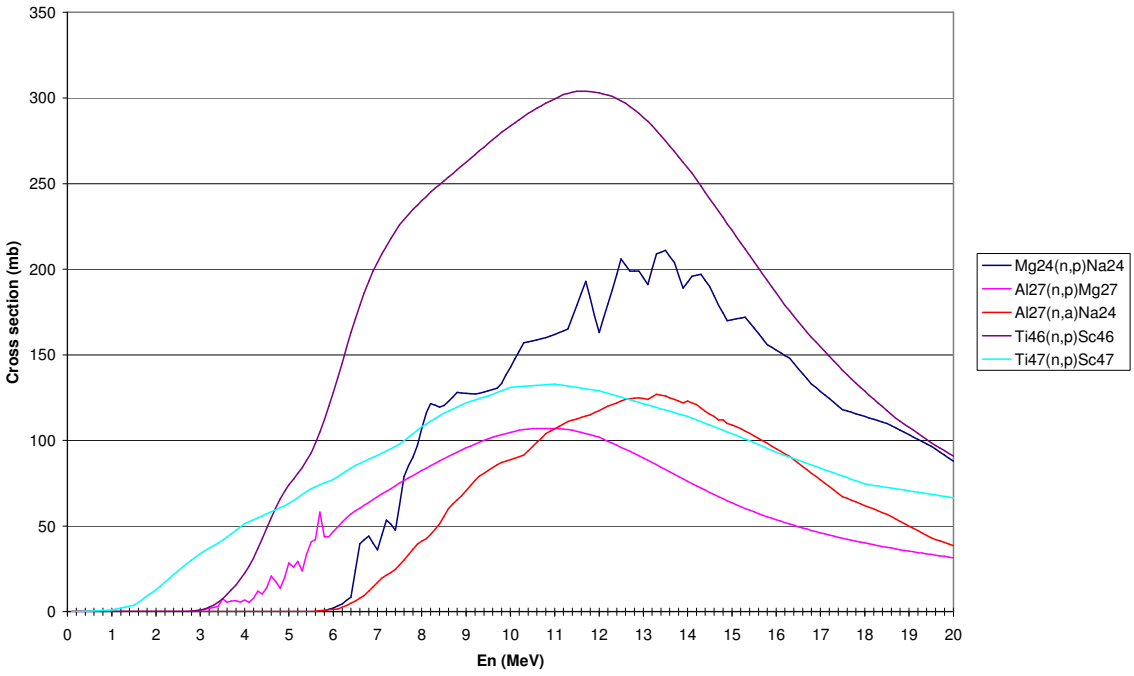

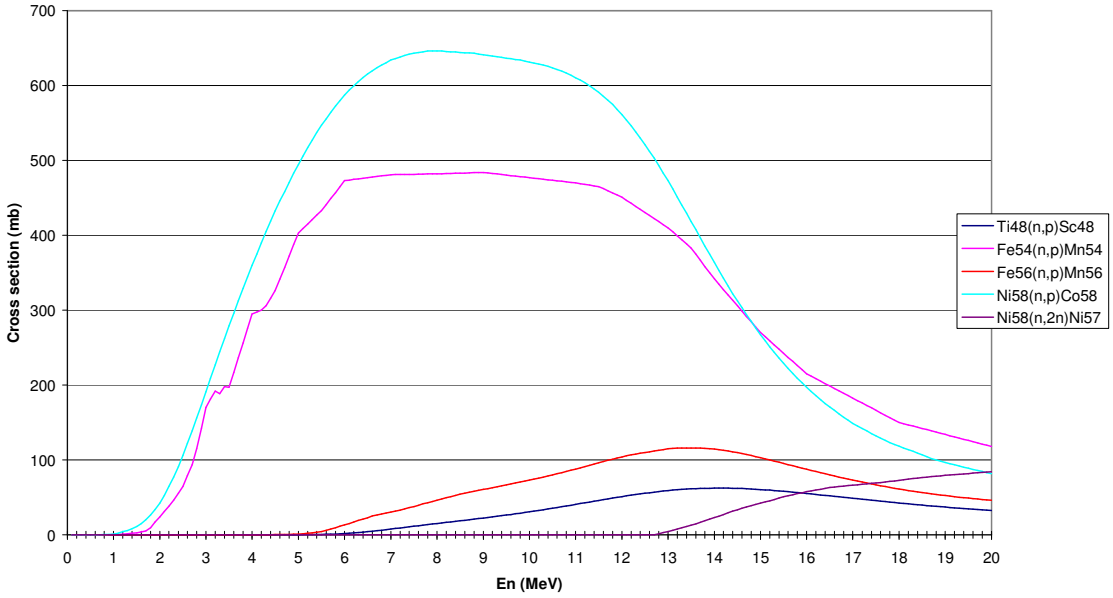

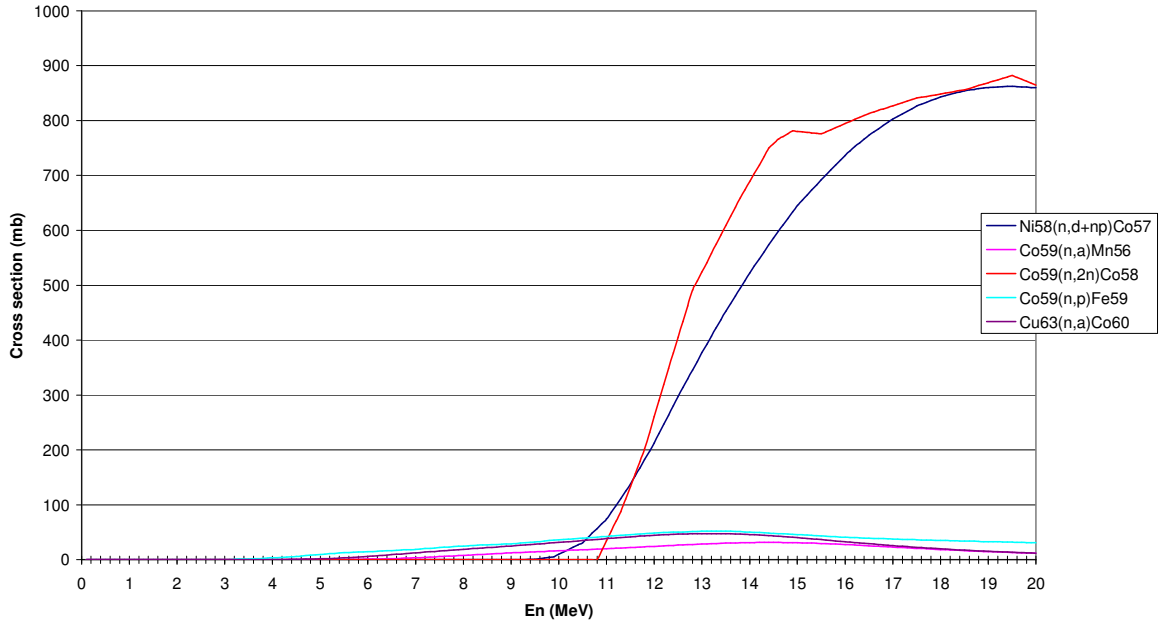
Cross section (mb)
En (MeV)
Ni58(n,d+np)Co57
Co59(n,a)Mn56
Co59(n,2n)Co58
Co59(n,p)Fe59
Cu63(n,a)Co60

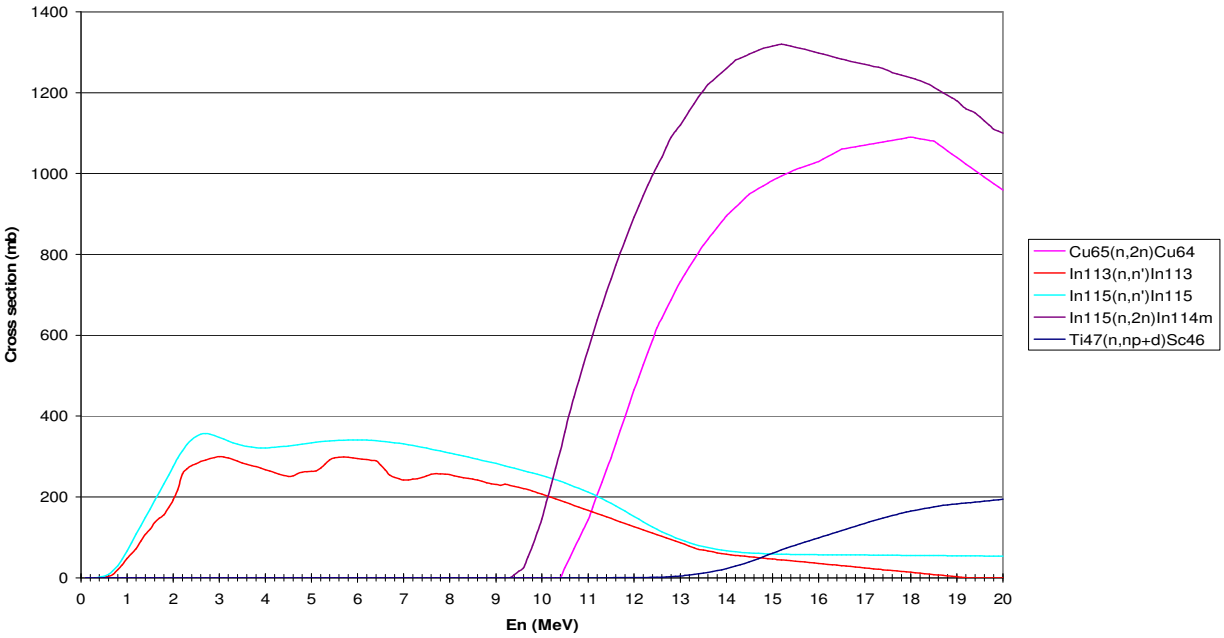
Cross section (mb)
En (MeV)
Cu65(n,2n)Cu64
In113(n,n')In113
In115(n,n')In115
In115(n,2n)In114m
Ti47(n,np+d)Sc46

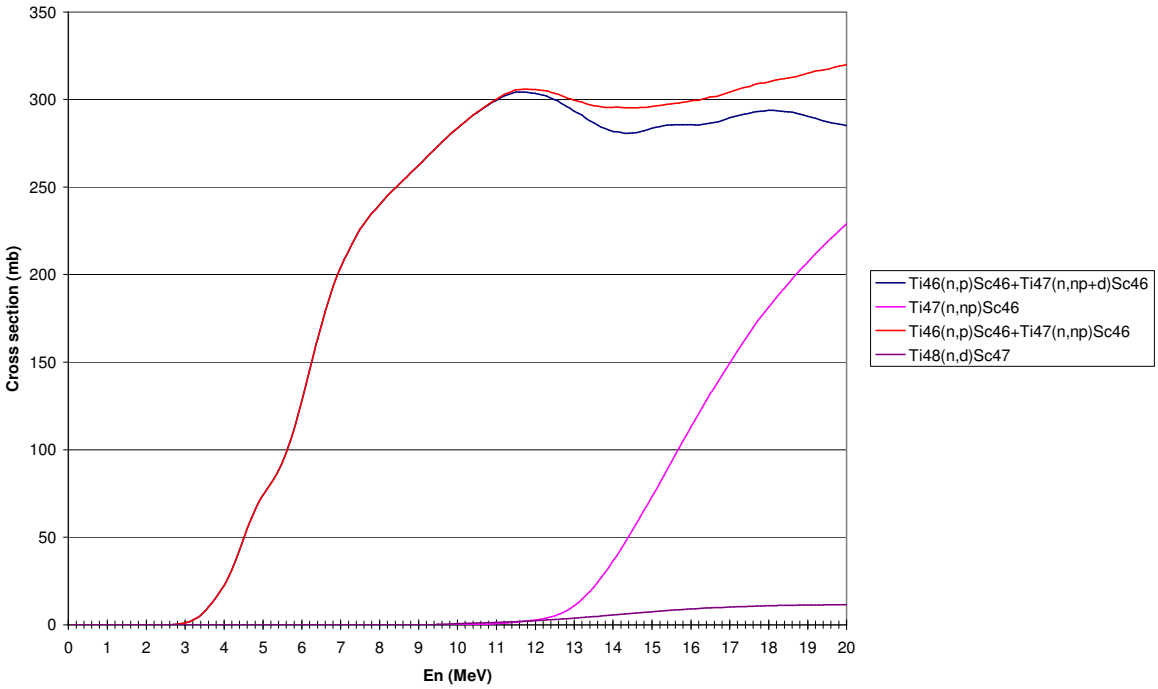
Cross section (mb)
En (MeV)
Ti46(n,p)Sc46+Ti47(n,np+d)Sc46
Ti47(n,np)Sc46
Ti46(n,p)Sc46+Ti47(n,np)Sc46
Ti48(n,d)Sc47

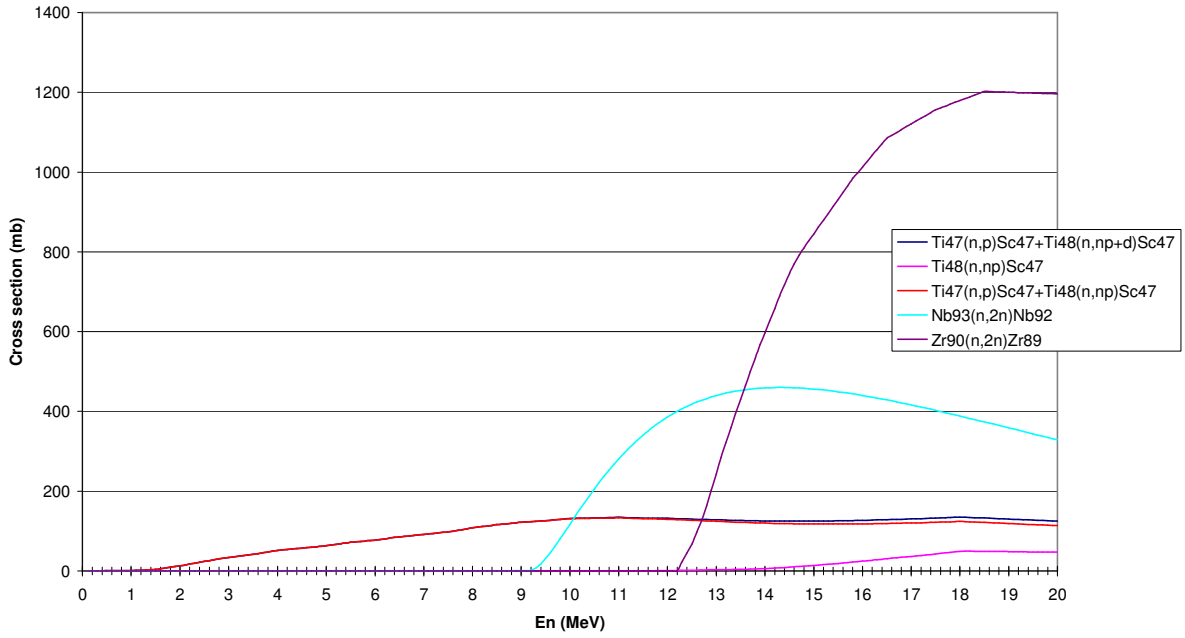
Cross section (mb)
En (MeV)
Ti47(n,p)Sc47+Ti48(n,np+d)Sc47
Ti48(n,np)Sc47
Ti47(n,p)Sc47+Ti48(n,np)Sc47
Nb93(n,2n)Nb92
Zr90(n,2n)Zr89

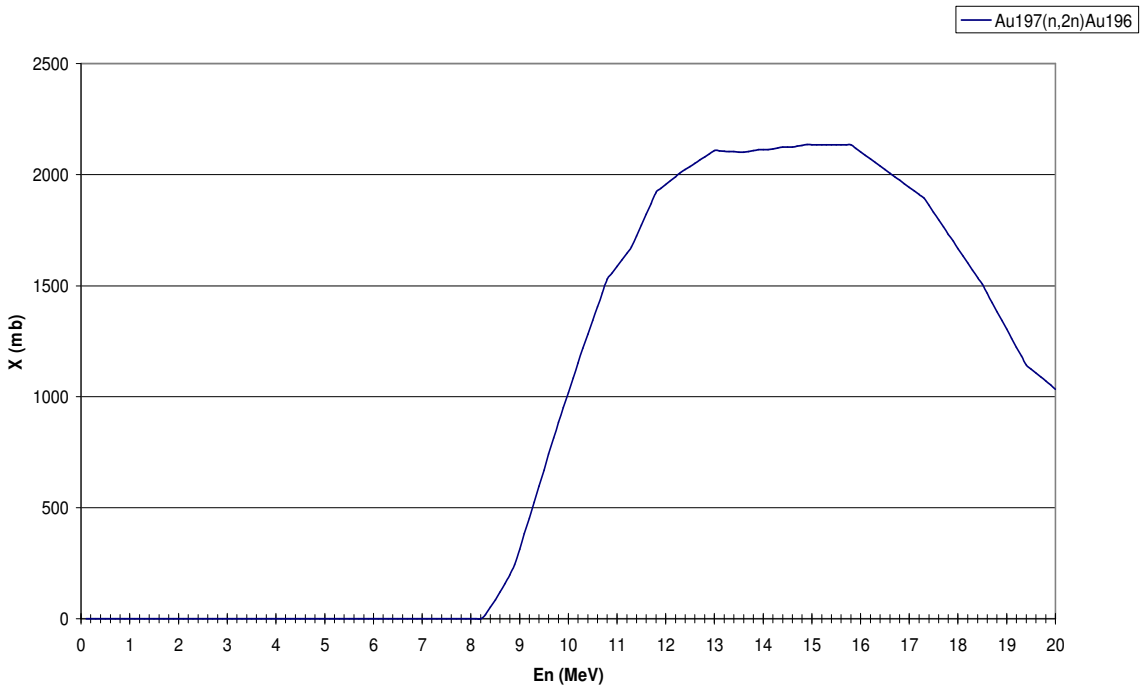
Au197(n,2n)Au196
X (mb)
2500
2000
1500
1000
500
0
0 1 2 3 4 5 6 7 8 9 10 11 12 13 14 15 16 17 18 19 20
En (MeV)

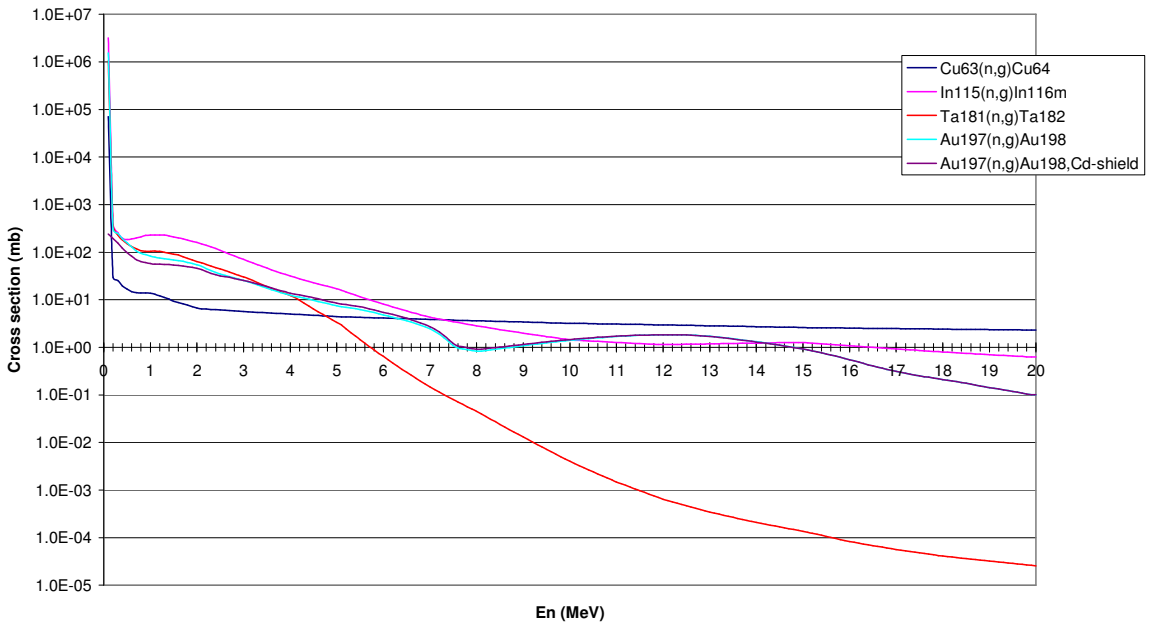
Cu63(n,g)Cu64
In115(n,g)In116m
Ta181(n,g)Ta182
Au197(n,g)Au198
Au197(n,g)Au198,Cd-shield
Cross section (mb)
1.0E+07
1.0E+06
1.0E+05
1.0E+04
1.0E+03
1.0E+02
1.0E+01
1.0E+00
1.0E-01
1.0E-02
1.0E-03
1.0E-04
1.0E-05
0 1 2 3 4 5 6 7 8 9 10 11 12 13 14 15 16 17 18 19 20
En (MeV)

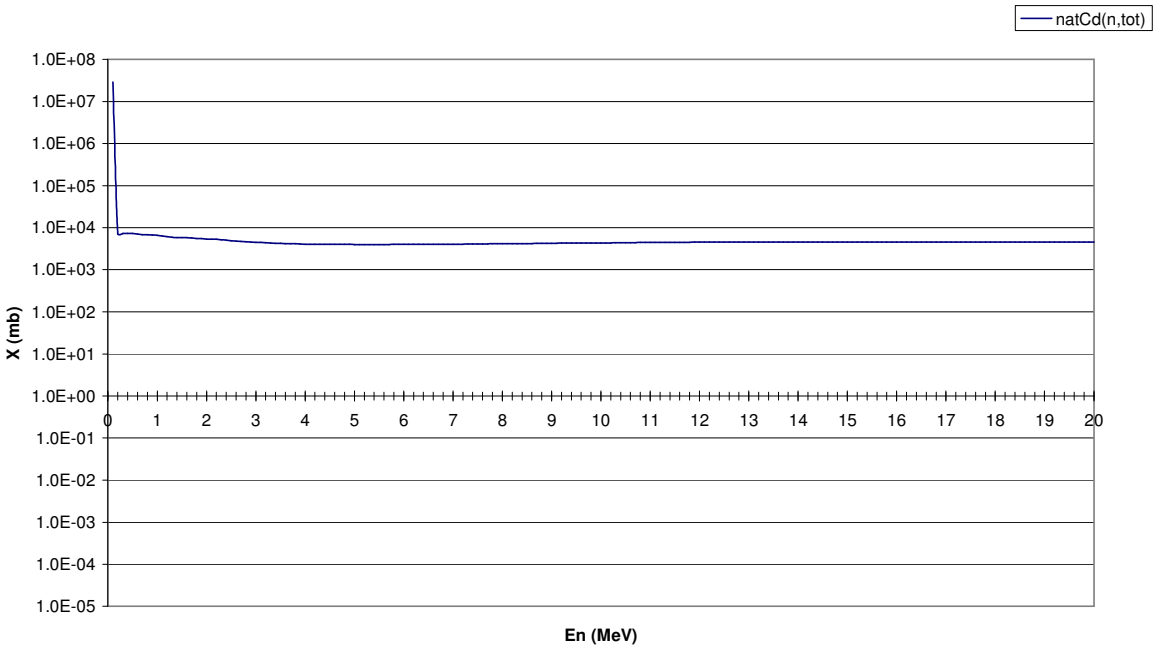
natCd(n,tot)
1.0E+08
1.0E+07
1.0E+06
1.0E+05
1.0E+04
1.0E+03
1.0E+02
1.0E+01
1.0E+00
1.0E-01
1.0E-02
1.0E-03
1.0E-04
1.0E-05
X (mb)
0 1 2 3 4 5 6 7 8 9 10 11 12 13 14 15 16 17 18 19 20
En (MeV)

Appendix 2

Operational neutron fluence spectra included in the WinDONA data base (from [IA-01])

TABLE 4-IX. Pu-238-Li Radioactie Neutron Sources
- Column 2: PU-LI SOURCE, UNSHIELDED
- Column 3: PU-LI SOURCE, SHIELDED BY 30 CM LIGHT WATER
- Column 4: PU-LI SOURCE, SHIELDED BY 30 CM HEAVY WATER

TABLE 4-VII. Cf-252
- Column 2: BARE 252 CF
- Column 3: 252 CF IN 15CM RADIUS D2O SPHERE
- Column 4: 252 CF IN 10.16CM RADIUS CH2 SPHERE
- Column 5: 252 CF IN 22.86CM RADIUS CH2 SPHERE
- Column 6: AS COLUMN 5 WITH 10.2CM THICK FE COVER

TABLE 4-VIII. Am-241 RADIOACTIVE NEUTRON SOURCES
- Column 2: AM-F SOURCE
- Column 3: AM-B SOURCE
- Column 4: AM-BE SOURCE
- Column 5: AM-LI SOURCE

TABLE 4-X. Alpha-Be Radioactive Neutron Sources
- Column 2: Accelerator epithermal beam
- Column 3: CM-BE SOURCE
- Column 4: PO-BE SOURCE
- Column 5: PU-BE SOURCE
- Column 6: RA-BE SOURCE

TABLE 4-XI. Photo Neutron Sorces
- Column 2: 140-LA-BE SOURCE
- Column 3: 116-IN-BE SOURCE
- Column 4: 24-NA-BE SOURCE
- Column 5: 24-NA-D2O SOURCE

TABLE 4-XIII. Intermediate Energy eutron Fields
- Column 2: NBS - ISNF/CV SPECTRUM
- Column 3: LOW FLUX RECTOR (LFR) SPECTRUM
- Column 4: SIGMA-SIGMA SPECTRUM
- Column 5: FILTERED BEAM OF CRIP LW REACTOR

TABLE 4-XIV. Heath Physics Research Reactor
- Column 2: HPRR, UNSHIELDED
- Column 3: HPRR, THROUGH 12 CM LUCITE
- Column 4: HPRR, THROUGH 13 CM STEEL
- Column 5: HPRR, THROUGH 20 CM CONCRETE
- Column 6: HPRR, THROUGH 5 CM STEEL + 15 CM CONCRETE

TABLE 4-XIX. Cf-252 and 239-Pu-Be Sources, Room Scatter and Skyshine
- Column 2: PU-BE, ROOM SCATTER
- Column 3: PU-BE, SKYSHINE
- Column 4: 252CF, ROOM SCATTER
- Column 5: 252CF, SKYSHINE

TABLE 4-XVI. Standard Reactor Fields, Set 1
- Column 2: VIPER REACTOR
- Column 3: JEZEBEL REACTOR
- Column 4: FLATTOP REACTOR
- Column 5: IBR-30, 68.5 M FAR FROM THE CORE
- Column 6: IBR-30, 8.8 M FAR FROM THE CORE

TABLE 4-XVII. Standard Reactor Fields, Set 2
- Column 2: STEK 4000, SPECTRUM NO. 9
- Column 3: NISUS SPECTRUM
- Column 4: ISNF-1 SPECTRUM
- Column 5: CFRMF SPECTRUM
- Column 6: YOPP SPECTRUM

TABLE 4-XX. hotons on Tungsten, Room Scatter and Skyshine
- Column 2: 25 MEV PHOTONS ON TUNGSTEN, ROOM SCATTER
- Column 3: 25 MEV PHOTONS ON TUNGSTEN, SKYSHINE
- Column 4: 14 MEV PHOTONS ON TUNGSTEN, ROOM SCATTER
- Column 5: 14 MEV PHOTONS ON TUNGSTEN, SKYSHINE

TABLE 4-XXI. Skyshine
Column 2: 650 MEV ELECTRON SYNCHROTRON SKYSHINE AT 24
Column 3: 650 MEV ELECTRON SYNCHROTRON SKYSHINE AT 110
Column 4: 650 MEV ELECTRON SYNCHROTRON SKYSHINE AT 300
Column 5: 14 MEV SKYSHINE THROUGH 1176 M AIR
Column 6: YAYOI SKYSHINE

TABLE 4-XXVII. Standard Reactor Fields, Set 3
Column 2: PURE FISSION SPECTRUM
Column 3: GODIVA SPECTRUM
Column 4: BIG-TEN SPECTRUM
Column 5: YAYOI SPECTRUM
Column 6: TAPIRO SPECTRUM

TABLE 5-IX. PWRs, Set 2 (old Compendium)
Column 2: P.W.R. LOCATION 6/R-2
Column 3: P.W.R. LOCATION 2/E-1
Column 4: P.W.R. LOCATION 3/E-2
Column 5: P.W.R. LOCATION 4/E-3
Column 6: P.W.R. LOCATION 6/R-3

TABLE 5-VII.BWR und PWRs (old Compendium)
Column 2: B.W.R. LOCATION E/3-X29
Column 3: P.W.R. LOCATION F/5
Column 4: P.W.R. LOCATION G/3
Column 5: P.W.R. LOCATION H/12

TABLE 5-VIII. PWRs, SET 1 (old Compendium)
Column 2: P.W.R. LOCATION I/1-I.V.
Column 3: P.W.R. LOCATION I/1-R.V.
Column 4: P.W.R. LOCATION J/3
Column 5: P.W.R. LOCATION 2/E-2
Column 6: P.W.R. LOCATION 3/E-3

TABLE 5-X. PWRs, Set 3 (old Compendium)
Column 2: P.W.R. LOCATION 2/L-2
Column 3: P.W.R. LOCATION 1/L-1
Column 4: P.W.R. LOCATION 3/L-3
Column 5: P.W.R. LOCATION 3/R-3

TABLE 5-XI. PWRs, Set 4 (old Compendium)
Column 2: P.W.R. LOCATION C'
Column 3: P.W.R. LOCATION 81
Column 4: P.W.R. LOCATION ORVCB
Column 5: P.W.R. LOCATION 9
Column 6: P.W.R. AT PAKS

TABLE 5-XII. PHWRs, (old Compendium)
Column 2: P.H.W.R. LOCATION REACTOR VAULT
Column 3: P.H.W.R. LOCATION 1
Column 4: P.H.W.R. LOCATION 4
Column 5: P.H.W.R. LOCATION FM S RM

TABLE 5-XIII. Medical Accelerators, Set 1 (old Compendium)
Column 2: 14 MEV PHOTONS ON TUNGSTEN
Column 3: 14 MEV PHOTONS ON TUNGSTEN THROUGH 90 CM CON
Column 4: 15 MEV PHOTONS ON TUNGSTEN
Column 5: 15 MEV PHOTONS ON TUNGSTEN THROUGH 90 CM CON

TABLE 5-XIV. Medical Accelerators, Set 2 (old Compendium)
Column 2: 18 MEV PHOTONS ON TUNGSTEN
Column 3: 18 MEV PHOTONS ON TUNGSTEN THROUGH 90 CM CON
Column 4: 25 MEV PHOTONS ON LEAD
Column 5: 25 MEV PHOTONS ON TUNGSTEN

TABLE 5-XIX. Synchrotrons (old Compendium)
Column 2: 650 MEV ELECTRON SYNCHROTRON
Column 3: SYNCHROPHASOTRON, LOCATION T.1
Column 4: SYNCHROCYCLOTRON, LOCATION T.1
Column 5: SYNCHROPHASOTRON, LOCATION T.2

TABLE 5-XV. Medical Accelerators, Set 3 (old Compendium)
Column 2: THERAC 40/SAGITTAIRE, INSIDE DOOR
Column 3: THERAC 40/SAGITTAIRE, OUTSIDE DOOR 1
Column 4: THERAC 40/SAGITTAIRE, OUTSIDE DOOR 2
Column 5: THERAC 40/SAGITTAIRE, LOCATION A

TABLE 5-XVI. Medical Accelerators, Set 4 (old Compendium)
Column 2: THERAC 40/SAGITTAIRE, LOCATION B
Column 3: THERAC 40/SAGITTAIRE, LOCATION C
Column 4: THERAC 40/SAGITTAIRE, LOCATION D
Column 5: THERAC 40/SAGITTAIRE, LOCATION E

TABLE 5-XVII. Medical Accelerators, Set 5 (old Compendium)
Column 2: U-120 CYCLOTRON, UNSHIELDED
Column 3: U-120 CYCLOTRON, SPECTRUM THROUGH 10 CM H2O
Column 4: U-120 CYCLOTRON, SPECTRUM THROUGH 10 CM CH2
Column 5: U-120 CYCLOTRON, SPECTRUM THROUGH 10 CM FE

TABLE 5-XX. MP Tandem Van De Graaff Stray Neutron, SET 1
Column 2: SITE 2
Column 3: SITE 4
Column 4: SITE 6
Column 5: SITE 8-V

TABLE 5-XXI. MP Tandem Van De Graaff Stray Neutron, SET 2
Column 2: SITE 11
Column 3: SITE 11-V
Column 4: SITE 12-V
Column 5: SITE 14

TABLE 5-XXII. High Energy Accelerators SET 1 (Old Compendium)
Column 2: ALTERNATING GRADIENT SYNCHROTRON
Column 3: STANFORD MARK III.
Column 4: COSMOTRON
Column 5: COSMOTRON (EXTENDED)
Column 6: CAL. TECH. SYNCHROTRON

TABLE 5-XXIV. High Energy Accelerators SET 3 (Old Compendium)
Column 2: NIMROD, LOCATION X2
Column 3: NIMROD, LOCATION P1
Column 4: 50 MEV LINAC PLA
Column 5: BROOKHAVEN LINAC, BLIP-I
Column 6: BROOKHAVEN LINAC, BLIP-II

TABLE 5-XXIX. Leakages (Old Compendium)
Column 2: STANFORD MARK III
Column 3: 1 GEV ELECTRON SYNCHROTRON
Column 4: BROOKHAVEN 3 GEV COSMOTRON

TABLE 5-XXV. High Energy Accelerators SET 4 (Old Compendium)
Column 2: AGS SOIL SHIELDED RING TOP
Column 3: WATER SHIELD FROM 200 MEV PROTON INTERECTION
Column 4: AGS RING TOP
Column 5: CYCLOTRON D-A1

TABLE 5-XXVI. Bevatrons, SET 1 (Old Compendium)
Column 2: LOCATION B-25/D
Column 3: LOCATION B-27/D
Column 4: LOCATION B-28/D
Column 5: LOCATION B-31/D

TABLE 5-XXX. Accelerator Shielded by Earth and Fe (Old Compendi
Column 2: 100 G/CM2 EARTH + H2O
Column 3: 1000 G/CM2 EARTH + H2O
Column 4: 2000 G/CM2 EARTH + H2O
Column 5: 2000 G/CM2 FE

TABLE 5-XXXI. Nuclear Materials Processing Facilitis (Old Compe
Column 2: 5 TON NATURAL URANIUM PILE
Column 3: CM203 POWER SOURCE
Column 4: PUF4 SOURCE
Column 5: TURKEY POINT, FUEL ELEMENT AT 14 INCHES
Column 6: TURKEY POINT, FUEL ELEMENT AT 26 INCHES

TABLE 5-XVIII. Fusion Reactors (old Compendium)
Column 2: TOKAMAK FUSION TEST REACTOR, ROOF
Column 3: TOKAMAK FUSION TEST REACTOR, WALL
Column 4: ORNL EXP. POWER REACTOR, FIRST WALL
Column 5: TOKAMAK, FIRST WALL
Column 6: 14 MEV STREAMING, LOCATION 4

TABLE 5-XXIII. High Energy Accelerators SET 2 (Old Compendium)
Column 2: CERN RING TOP
Column 3: CERN SYNCHROTRON BRIDGE
Column 4: LBL BEVATRON

TABLE 5-XXVII. Bevatrons, SET 2 (Old Compendium)
Column 2: LOCATION B-39/D
Column 3: LOCATION B-40/D
Column 4: LOCATION B-41/D
Column 5: LOCATION B-43/D

TABLE 5-XXXII. Bare and Moderated 238-Pu -1 8-O-2 (Old Compendi
Column 2: BARE 238-PU - 18-O-2 SOURCE
Column 3: MODERATED BY 7.6 CM DIAM. CH2 SPHERE
Column 4: MODERATED BY 12.7 CM DIAM. CH2 SPHERE
Column 5: MODERATED BY 20.3 CM DIAM. CH2 SPHERE
Column 6: MODERATED BY 25.4 CM DIAM. CH2 SPHERE

TABLE 5-XXXIV. Cosmic Rays, Set 2 (Old Compendium)
Column 2: COSMIC RAY SPEC
Column 3: COSMIC RAY SPECT
Column 4: COSMIC RAY SPECTRUM AT TOP
Column 5: COSMIC RAY SPECT

TABLE 4-IX. Am-Be SPECTRA AVAILABLE AT PTB
Column 2: The Difference
Column 3: Measured with shadow cone
Column 4: Measured without shadow cone

TABLE 4-V. REFERENCE SPECTRA, RECOMMENDED BY ISO-8529
Column 2: CF252, ISO
Column 3: D2O MOD. CF, ISO
Column 4: AMBE, ISO
Column 5: AMB, ISO

TABLE 4-VI. BARE CF SPECTRA AVAILABLE AT PTB
Column 2: Measured without shadow cone
Column 3: Measured with shadow cone
Column 4: The difference

TABLE 4-VII. HEAVY WATER MODERATED CF SPECTRA AVAILABLE AT PT
Column 2: Measured without shadow cone
Column 3: Measured with shadow cone
Column 4: The difference

TABLE 4-VIII. MODERATED CF SPECTRA AT TOHOTO UNIV. AND DUBNA
Column 2: Iron moderated Cf
Column 3: Carbon moderated Cf
Column 4: Polyethylene moderated Cf
Column 5: Polyethylene moderated Cf, D=29.2 cm
Column 6: Polyethylene moderated Cf, D=12.7 cm

TABLE 4-X. Pu-Be CALIBRATION SPECTRA AVAILABLE AT CERN
Column 2: In 1 m distance
Column 3: In 2 m distance
Column 4: In 3 m distance
Column 5: Shielded by PE, in 1 m distance
Column 6: Shielded by PE, in 2 m distance

TABLE 4-XI. PLUTONIUM SPECTRA AVAILABLE AT LLL AND PNL, RICHLAND
Column 2: Bare Pu-Be source, room scatter
Column 3: H2O moderated Pu-Be, R=25 cm, room scatter
Column 4: D2O moderated Pu-Be, R=25 cm, room scatter
Column 5: Bare PuO2 at 100 cm
Column 6: Bare Pu metal at 50 cm

TABLE 4-XII. PLUTONIUM-FLUORID SPECTRA AVAILABLE AT PNL, RICHLAN
Column 2: Bare at 50 cm
Column 3: 1" Acrylic moderated at 50 cm
Column 4: 2" Acrylic moderated at 50 cm
Column 5: Bare at 100 cm
Column 6: 2" Acrylic moderated at 100 cm

TABLE 4-XIII. MODERATED CF SPECTRA AVAILABLE AT NRI, REZ
Column 2: Cf + 5 cm Fe, 10 cm PE
Column 3: Cf + 25 cm Fe, 10 cm PE

Column 4: Cf + 5 cm Fe
Column 5: Cf + 25 cm Fe

TABLE 4-XIV. SIMULATION OF WORK PLACE SPECTRA AT CADARACHE AND G
Column 2: Cadarache, spectrum 1
Column 3: Cadarache, spectrum 2
Column 4: Grenf facility, pos. A
Column 5: Grenf facility, pos. B
Column 6: Grenf facility, pos. C

TABLE 4-XIX. SIMULATION OF FISSION ENVIRONMENT (UTR-KINKI FACILI
Column 2: Central Void
Column 3: Central Void + Fission plate
Column 4: Central Void + fission plate + boron

TABLE 4-XV. SIMULATION OF WORK PLACE SPECTRA AT GSF AND PTB
Column 2: GSF GRENF, 30 cm D2O sphere
Column 3: GSF GRENF, 10 cm Fe slab
Column 4: GSF GRENF, 10 cm PE slab
Column 5: PTB, Li(p,n)Be, 2.5 MeV
Column 6: PTB, Li(p,n)Be, 3.3 MeV

TABLE 4-XVI. SIMULATION OF WORK PLACE SPECTRA USING U-238 IN CAD
Column 2: 2.8 MeV neutrons on 238-U, no duct
Column 3: 2.8 MeV neutrons on U-238, with PE duct
Column 4: 2.8 MeV neutrons on 238-U, with duct + 1 cm
Column 5: Reference spectrum at TRU facility
Column 6: 3MeV neutrons on 238-U, with duct + 10 cm H

TABLE 4-XVII. SIMULATION OF WORKPLACE SPECTRA IN CADARACHE, 14 M
Column 2: PE duct + 5 cm D20 shield
Column 3: Simulated fuel transport container
Column 4: Bare beam
Column 5: 5 cm H2O shield
Column 6: 20 cm H2O shield

TABLE 4-XVIII. SIMULATION OF FUSION ENVIRONMENT (TEXTOR)
Column 2: in the beam
Column 3: with iron shield
Column 4: with wooden shield, pos.1
Column 5: with wooden shield, pos.2

TABLE 4-XX. SIMULATION OF STRAY NEUTRON FIELDS AT SILENE REACTOR
Column 2: unmoderated spectrum
Column 3: lead shield
Column 4: PE shield
Column 5: steel shield

TABLE 4-XXI. SIMULATION OF STRAY NEUTRON FIELDS AT A PWR
Column 2: Experimental pos. 1
Column 3: Experimental pos. 2
Column 4: MOX element container

TABLE 4-XXII. HIGH ENERGY REFERENCE SPECTRA AT PSI AND CERN
Column 2: PSI, 60 MeV, Pure beam
Column 3: PSI, 60 MeV, Background
Column 4: PSI, 60 MeV, Beam with background
Column 5: CERN, lead beam on lead
Column 6: CERN, concrete shield, proton beam on copper

TABLE 4-XXIV. HIGH ENERGY REFERENCE SPECTRA AT CERN, FFTP, SSRL
Column 2: CERN-CEC, Iron shield
Column 3: CERN-CEC, Concrete shield
Column 4: FFTP facility
Column 5: SSRL Linac, diagnostic room
Column 6: SSRL SPEAR, on the roof

TABLE 4-XXV. HIGH ENERGY REFERENCE SPECTRA AT JINR AND IHEP
Column 2: Phasotron, Soft field
Column 3: Phasotron, Hard field
Column 4: IHEP, filtered by 220 cm concrete

TABLE 4-XXIII. HIGH ENERGY REFERENCE SPECTRA AT CERN
Column 2: Concrete top
Column 3: Concrete side
Column 4: Iron top
Column 5: Iron side

TABLE 5-IX. CAORSO, BWR, CALCULATED
Column 2: Position 1
Column 3: Position 2
Column 4: Position 3
Column 5: Position 4

TABLE 5-VIII. CAORSO, BWR, MEASURED
Column 2: Position 1
Column 3: Position 2
Column 4: Position 3
Column 5: Position 4

TABLE 5-X. MEASURED BWR AND PWR SPECTRA (U.K.)
Column 2: DUNGBCFL, in Boiler Cell
Column 3: DUNGRFFL, Roof
Column 4: DUNGWWFL, Walkway
Column 5: PWR1GOFL, Position 1
Column 6: PWR2GOFL, Position 2

TABLE 5-XI. MEASURED PWR SPECTRA (U.K.)
Column 2: TRAWSFYNYDD, Filter galery
Column 3: HINKLEY POINT, Pile cap
Column 4: HINKLEY POINT, Filter galery

TABLE 5-XII. MEASURED PWR SPECTRA (WOLF CREEK)
Column 2: Power 50%, PH 2047'Level
Column 3: Power 50%, PH 2047'
Column 4: Power 50%, 2026' Level by Valves
Column 5: Power 100%, PH
Column 6: Power 100%, 2026' A Loop Penetration

TABLE 5-XIII. CZECH PWR, PUMPS' ROOM
Column 2: near cold side
Column 3: between pump & cold side
Column 4: hot side
Column 5: near entrance door
Column 6: between pumps 3 & 4

TABLE 5-XIV. CZECH PWR, VESSEL TEST ROOM
Column 2: under reactor, pos.1
Column 3: middle of room
Column 4: under reactor, pos.2
Column 5: corridor outside room

TABLE 5-XIX. SWISS BWR, MARK I, 1
Column 2: Maze entrance
Column 3: 1st bend of maze
Column 4: Entrance of drywell
Column 5: Under access opening
Column 6: Btw. drywell & stairwell

TABLE 5-XL. REACTOR FUEL TREATMENT, Pu REPROCESSING PLANT (USA)
Column 2: Lightly shielded
Column 3: Heavily shielded
Column 4: Operator desk
Column 5: At conduit exit
Column 6: At glove box

TABLE 5-XLI. ISOTOPIC SOURCE PRODUCTION
Column 2: AmO2 in container
Column 3: Cm244 bare, in glove box
Column 4: Am-Be bare, in glove box
Column 5: Am ceramic discs

TABLE 5-XLII. BORON THERAPY, 1
Column 2: Petten HB11 filtered beam
Column 3: Accelerator based spectrum
Column 4: Gantry, cell 55
Column 5: LVR-15 epithermal beam, BS meas.

TABLE 5-XLIV. BORON THERAPY SPECTRA, 3
Column 2: Accelerator epithermal beam
Column 3: BMRR beam
Column 4: Accelerator, filtered by AL/ALF3
Column 5: Accelerator, filtered by 7LiF
Column 6 :Accelerator, filtered by D2O

TABLE 5-XLIII. BORON THERAPY SPECTRA, 2
Column 2: Spallation source
Column 3: RENT I beam
Column 4: FRM II unfiltered
Column 5: FRM II filtered

TABLE 5-XV. CZECH PWR, REACTOR HALL
Column 2: above reactor cap
Column 3: above isolation valve
Column 4: above steam generator
Column 5: platform of reactor cap

TABLE 5-XVI. PWR, IN CONTAINMENT (USA)
Column 2: Site 5
Column 3: Site 6 (SPUNIT code)
Column 4: Site 4 (SPUNIT code)
Column 5: Site 4 (YOGI code)

TABLE 5-XVII. RINGHALS, SWEDEN
Column 2: CLAB at point D
Column 3: CLAB at point E
Column 4: CLAB at point P
Column 5: B4 at point L
Column 6: B2 at point G

TABLE 5-XVIII. GAS COOLED (U.K.)
Column 2: Position CH1
Column 3: Position CH2
Column 4: Filter galery pos. S3
Column 5: Filter galery pos. S4

TABLE 5-XX. SWISS BWR, MARK I, 2
Column 2: 16m level, near pump
Column 3: 16 m level, near sprinkler tap
Column 4: Containment lock, door closed
Column 5: Containment lock, door open

TABLE 5-XXI. SWISS PWR, WESTINGHOUSE
Column 2: 1m from metal door into containment
Column 3: In containment, 1m from platform
Column 4: In containment, 3m from platfrom
Column 5: behind steam generator

TABLE 5-XXII. SWISS PWR, SIEMENS KWU
Column 2: 18.4 m level, reactor axis
Column 3: reactor level, 40 cm behind metal door
Column 4: reactor level, 33 cm behind metal door

TABLE 5-XXIV. MICROTRON STRAY FIELD, 2
Column 2: Site E, door 2 open
Column 3: Site E, door 2 closed
Column 4: Site D, with backing, door 2 closed
Column 5: Site D, without backing, door 2 closed
Column 6: Site D, door 2 open

TABLE 5-XXVIX. TOKYO UNIV. 1 GEV SYNCHROTRON
Column 2: Skyshine at 111m, calculated
Column 3: Skyshine at 111m, measured
Column 4: On concrete roof, calculated
Column 5: On concrete roof, measured
Column 6: Model spectrum for skyshine calculation

TABLE 5-XXV. AVF, TOHOKO UNIV. 35 MEV CYCLOTRON, 1
Column 2: Cyclotron room
Column 3: 1st leg of labyrinth
Column 4: 2nd leg of labyrinth, pos. 1
Column 5: 2nd leg of labyrinth, pos. 2
Column 6: 2nd leg of labyrinth, coupling interface

TABLE 5-XXVI. AVF, TOHOT UNIV. 35 MEV CYCLOTRON, 2
Column 2: 2nd leg of labyrinth, pos. 4
Column 3: 3rd leg of labyrinth, in front of iron door
Column 4: 3rd leg of labyrinth, behind iron door
Column 5: Underpath for room

TABLE 5-XXX. DESY LEAKAGE NEUTRON SPECTRA, 1
Column 2: Concrete shielding
Column 3: Heavy concrete shielding
Column 4: Iron shielding
Column 5: Iron and concrete shielding

TABLE 5-XXXI. DESY LEAKAGE NEURON SPECTRA, 2
Column 2: Sand + concrete
Column 3: Heavy concrete
Column 4: Heavy concrete, thin target
Column 5: Concrete, thick target

TABLE 5-XXXV. REACTOR FUEL TREATMENT, CASK 2
Column 2: NTL111 container, at 115 cm
Column 3: NTL111 container, at 367 cm
Column 4: 1392/1
Column 5: 1393/2

TABLE 5-XXIII. MICTROTRON STRAY FIELD, 1
Column 2: 1m from Au target
Column 3: Site B, measured
Column 4: Site C, measured
Column 5: Site D, door 2 open
Column 6: Site D, door 2 closed

TABLE 5-XXVII. TRIUMF, 500 MEV CYCLOTRON
Column 2: Vault door
Column 3: TNF door
Column 4: South of LD2 target
Column 5: M8 channel
Column 6: Top of TNF

TABLE 5-XXVIII. KEK, 12 GEV SYNCHROTRON
Column 2: Location 11
Column 3: Location 1
Column 4: Location 2
Column 5: Location 5
Column 6: Location 4

TABLE 5-XXXII. 46 MEV CYCLOTRON STRAY NEUTRON SPECTRA
Column 2: Variable energy port, START1 start sp.
Column 3: Variable energy port, FLAT start sp.
Column 4: Variable energy port, GRAVES start sp.
Column 5: Variable energy port, Maxwellian start sp.
Column 6: Switching magnet, Maxwellian start sp.

TABLE 5-XXXIII. COSMIC RAY SPECTRA, MEASURED AND CALCULATED
Column 2: PTB, Free in air
Column 3: PTB, in basement
Column 4: At 5000 m above ROME, Luin code
Column 5: Zugspitze by FLUKA code
Column 6: Zugspitze measured

TABLE 5-XXXIV. REACTOR FUEL TREATMENT, CASK 1
Column 2: LK100 container, location 1
Column 3: TN12 container
Column 4: LK100 container, location 2
Column 5: PuF4 workstation in Valduc

TABLE 5-XXXIX. REACTOR FUEL TREATMENT, Pu REPROCESSING PLANT (U.
Column 2: Location 1
Column 3: Location 2
Column 4: Location 3
Column 5: Location 4
Column 6: Location 5

TABLE 5-XXXVI. REACTOR FUEL TREATMENT, CASK 3 (WWR)
Column 2: Storage hall, at 0.45 m
Column 3: Storage hall, at 2 m
Column 4: Transport wagon, corridor, at 0.45 m
Column 5: Transport wagon, corridor, at 2 m

TABLE 5-XXXVII. REACTOR FUEL TREATMENT, MOX
Column 2: bare MOX fuel, at 20 cm
Column 3: MOX fuel in borated water
Column 4: MOX fuel, at storage place
Column 5: GSF MOX fuel cask, pos. 2
Column 6: GSF MOX fuel cask, pos. 3

TABLE 5-XXXVIII. REACTOR FUEL TREATMENT, FUEL STORAGE
Column 2: Hanau fuel storage, Bonner sphere
Column 3: Hanau fuel storage, NE213 spectrometer
Column 4: POLLUX container simulation, above ground
Column 5: POLLUX container simulation, underground

European Commission

EUR 23305 EN – Joint Research Centre – Institute for Reference Materials and Measurements
Title: DONA detector: further improvements and evaluation for field applications
Authors: G. Lövestam, A. Fessler, J. Gasparro, M. Hult, P. Kockerols, G. Marissens,
K. Okkinga, J.S.E. Wieslander
Luxembourg: Office for Official Publications of the European Communities
2007 – 30 pp. – 21.0 x 29.7 cm
EUR – Scientific and Technical Research series – ISSN 1018-5593
ISBN 978-92-79-08813-1

Abstract
The DONA neutron spectrometer concept is based on the measurement of neutron induced activity in a series of small metal disks that have been exposed to a neutron field. The induced activity is measured and the neutron spectrum is calculated using and unfolding technique, based on environmental neutron spectra. A complete measurement is performed in three steps: 1. Placement of the detector device (the holder with the metal disks) at the measurement site. 2. Transport of the detector to a gamma-ray measurement laboratory where the neutron induced activity is detected. 3. Calculation of the neutron intensity and spectrum using unfolding algorithms and an environmental neutron spectrum library.

The novelty of the approach lies in the concept as such, including usage of carefully selected metal disks arranged in a holder, high performance gamma-ray spectrometry and spectrum unfolding using a library of environmental neutron spectra. In 2004, a first study was carried out within the frame of an IRMM exploratory research project. Several detectors were developed and successfully tested in laboratory neutron fields. This report covers the IRMM exploratory research prolongation project for 2006 in which the same detector concept is used, however, now in environmental neutron fields with considerably lower neutron fluence rates. The result shows that after further refinement of the detector device and the data evaluation program the detector can very well be used for environmental neutron fluence measurements. Tests were done at PTB, Germany, using their calibrated neutron source and at the MOX fuel fabrication plant Belgonuclearire in Mol, Belgium.

The mission of the JRC is to provide customer-driven scientific and technical support for the conception, development, implementation and monitoring of EU policies. As a service of the European Commission, the JRC functions as a reference centre of science and technology for the Union. Close to the policy-making process, it serves the common interest of the Member States, while being independent of special interests, whether private or national.

JRC
EUROPEAN COMMISSION

LA- NA- 23305- EN- C

ISBN 978-92-79-08813-1